Geophys. J. Int. (2001) **146,** 249–263

The effects on seismic waves of interconnected nearly aligned cracks

S. R. Tod[1,2]

[1] *Department of Applied Mathematics and Theoretical Physics, University of Cambridge, Silver Street, Cambridge* CB3 9EW, *UK.*
E-mail: s.r.tod@damtp.cam.ac.uk
[2] *British Geological Survey, West Mains Road, Edinburgh,* EH9 3LA, *UK*

Accepted 2001 February 12. Received 2001 February 7; in original form 2000 August 22

SUMMARY

Transfer of fluid between connected cracks may occur during the passage of seismic waves. Such fluid flow can be modelled using an extension of effective medium theory (Hudson *et al.* 1996) and is effected via non-compliant pores. The flow is governed by a parameter τ representing the relaxation time of pressure equalization between cracks. However, if the cracks are fully aligned and have the same aspect ratio, the theory produces the unexpected result that, at low frequencies, the cracks are effectively isolated and at high frequencies they are fully drained. The artificial restriction of the model to perfectly aligned cracks of identical aspect ratio is seen to be the cause of this result. By reworking the model to allow the crack orientation and aspect ratios to vary, we see that a more realistic model has the usual properties in which the cracks are isolated at high frequencies and undrained at low frequencies. We have chosen the distributions of aspect ratios to be in agreement with observation (Hay *et al.* 1988). Thomsen's parameters (Thomsen 1986) and the attenuation coefficients are seen to be frequency-dependent via the non-dimensional parameter $\omega\tau$.

Key words: anisotropy, cracks, permeability, porosity.

1 INTRODUCTION

Cracking originates in rocks from a number of geological processes, of which thermal gradients and tectonic stress are particularly important. The resulting fracture network will depend upon both the mineralogy and grain orientation within the rock. Experiments on thermally induced cracking (Fredrich & Wong 1986; Hadley 1976; Homand-Etienne & Houpert 1989) and stress-induced cracking (Montoto *et al.* 1995; Tapponnier & Brace 1976; Wong 1982) suggest that the former process produces a fairly isotropic distribution of predominantly intergranular cracks, while the latter produces a strongly anisotropic distribution of intragranular and transgranular cracks, with the majority of cracks oriented parallel to the direction of maximum principal stress (David *et al.* 1999; Menéndez *et al.* 1999).

Effective medium theories giving expressions for the overall mechanical properties (in particular, the wave speeds) of materials with cracks are now well established. Among the best known are the self-consistent method (O'Connell & Budiansky 1974), the method of smoothing (Hudson 1980) and the differential method (Nishizawa 1982). In all such theories it is necessary to calculate the response of a single crack in an unbounded homogeneous matrix. Since all the methods involve extensive averaging, the cracks are represented for this purpose by a 'mean crack', usually taken to be circular. The cracks may be aligned, partially aligned or randomly oriented (Hudson 1986), they may be filled with gas (dry), liquid or a weak solid (Hudson 1981) and they may be connected through the porosity of the matrix rock (Hudson *et al.* 1996; O'Connell & Budiansky 1977). In the latter case, fluid is able to flow between cracks that, because of their difference in orientation, say, have been distorted differently by an imposed stress field. We follow the analysis of Hudson *et al.* (1996) here and it should be borne in mind that the theory developed here is valid only to first order in the number density of the cracks. Although Hudson *et al.* (1996) and Pointer *et al.* (2000) imply that the extension to second order in the number density is straightforward, it has not been established that this is the case and we restrict ourselves to a first-order theory here.

In their paper, Hudson *et al.* (1996) derived a rather unexpected result for aligned connected cracks. This was that, in high-frequency wave propagation, the cracks behave as if they are completely drained (dry) and, at low frequencies, as if they are isolated without connections. Although apparently running against physical intuition, this result is explained by the fact that because the cracks are fully aligned, the pressure gradient driving fluid from one crack to another varies on the scale of a wavelength, inversely proportional to the frequency ω; the diffusion length, on the other hand, varies as $\omega^{-1/2}$. Thus, as the frequency tends to zero, the diffusion is less and less effective, with the opposite effect as $\omega \to \infty$.

Hudson *et al.* (1996) derived their results for aligned cracks by a method that ignores local crack-to-crack flow since it was assumed that because the cracks all have the same orientation, it would be unimportant. However, if the formulae for non-aligned cracks are specialized to cracks with a single orientation, the result differs from the above in the addition of one term that becomes important at high frequencies. The incorporation of crack-to-crack flow shows that it cannot be neglected when the frequency is sufficiently high that the wavelength approaches the size of the intercrack spacing. We compare the two results here and show that, with the more complete theory, fully aligned cracks behave as if isolated at high frequencies as might be expected. However, they still behave as if isolated at very low frequencies for the reasons given above.

As well as depending on the assumption that the cracks are fully aligned, these results also rely on the fact that the cracks were assumed all to have the same aspect ratio. Relaxing either of these two assumptions leads to local fluid flow between neighbouring cracks that have been distorted in different ways by the incoming wave because of their different orientations or aspect ratios or both. In this paper we analyse the effect of allowing small variations in alignment and aspect ratio and find that the behaviour of the material is that of undrained cracks at low frequencies, in accordance with physical expectation. We show, graphically, how the material behaves when the cracks are nearly aligned and when they all have nearly the same aspect ratio.

2 BACKGROUND

The method of smoothing developed by Keller (1964) has been applied by Hudson (1980, 1981, 1986) to determine expressions for the effective elastic parameters $\mathbf{c}$ of a cracked material, to first order in crack density $\varepsilon = v^s \langle a^3 \rangle$, where $v^s = N/V$, N is the number of cracks, V is the material volume, a is the crack radius and the operator $\langle . \rangle$ denotes the mean value, such that

$$\mathbf{c} = \mathbf{c}^0 + \varepsilon \mathbf{c}^1 + \mathcal{O}(\varepsilon^2) , \tag{1}$$

where $\mathbf{c}^0$ is the elastic tensor for the assumed isotropic, porous matrix material,

$$c^0_{ipjq} = \lambda \delta_{ip} \delta_{jq} + \mu \left(\delta_{ij} \delta_{pq} + \delta_{iq} \delta_{jp} \right) , \tag{2}$$

where λ and μ are the Lamé constants of the material; $\mathbf{c}^1$ accounts for scattering off individual cracks.

Determination of $\mathbf{c}^1$ depends upon the orientation of the cracks and the nature of the crack infill. Expressions for $\mathbf{c}^1$ under varying conditions for isolated cracks can be found in Hudson (1980, 1981, 1986). For aligned isolated cracks of identical aspect ratio, with normals lying in the x_3-direction, these are of the form

$$c^1_{ipjq} = -\frac{1}{\mu} c^0_{k3ip} c^0_{l3jq} \bar{\mathcal{U}}_{kl} , \tag{3}$$

where the nature of the crack infill is reflected in the diagonal matrix $\{\bar{\mathcal{U}}_{kl}\}$, where $\bar{\mathcal{U}}_{11} = \bar{\mathcal{U}}_{22}$, due to the assumed symmetry of each crack. The resulting effective medium is vertically transversely isotropic.

3 THEORY

The model of connected cracks proposed by Hudson *et al.* (1996) for the transfer of fluid between cracks by non-compliant pores (seismically transparent pathways) (see Figs 1a and b) makes the assumptions that the distortion of the pores is negligible compared with that of the cracks during the passage of a wave and that the pore porosity is low, so that we neglect compression of the pore fluid.

The population of cracks is divided into families of parallel cracks with identical aspect ratio and identical radius, labelled $n = 1, 2, \ldots$. Hudson *et al.* (1996) give a first-order expression for the porosity of the nth set of cracks,

$$\phi_n = \phi^0_n + \boldsymbol{\phi}^1_n : (\boldsymbol{\sigma}^0 + p^n_{\mathrm{f}} \mathbf{I}) - \frac{\phi^0_n p^n_{\mathrm{f}}}{\kappa} , \tag{4}$$

where $\kappa = \lambda + 2\mu/3$ is the bulk modulus of the matrix material, ϕ^0_n and $\boldsymbol{\phi}^1_n$ are the stress-free porosity and the first-order dependence on stress, respectively, for the nth set of cracks, $\boldsymbol{\sigma}^0$ is the imposed static stress field and p^n_{f} is the fluid pressure in the nth set of cracks.

(a)

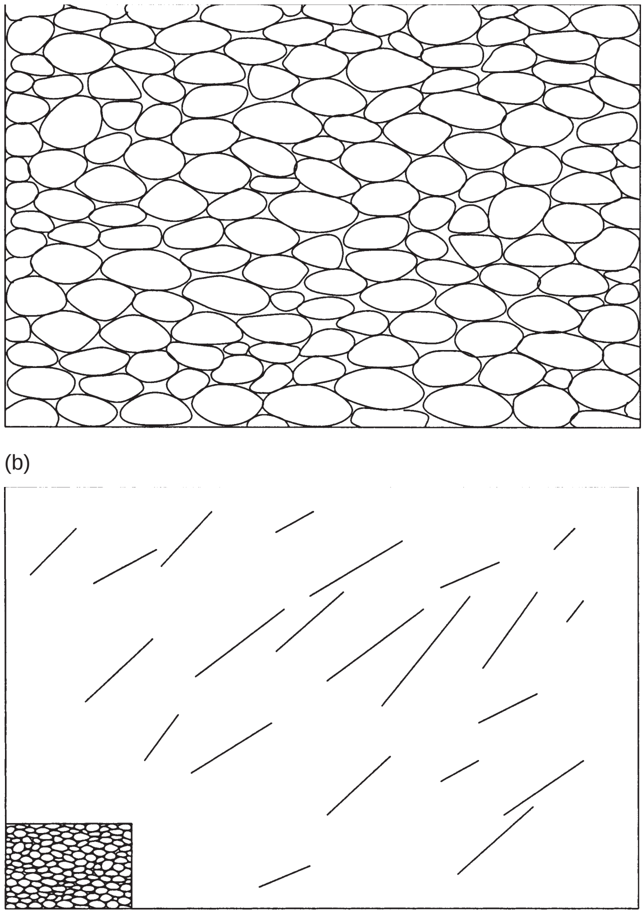

(b)

Figure 1. (a) Schematic of an aggregate in which the misfit between the particles creates a porous system. (b) Schematic of a possible distribution of nearly aligned cracks in an aggregate. The insert (a reduced version of a) represents the structure of the material in which the cracks lie.

The relation proposed by Hudson *et al.* (1996) for the mass flow out of the nth set of cracks, derived in Appendix A, is

$$\frac{\partial(\rho_f^n \phi_n)}{\partial t} = -\frac{\phi_n^0 \rho_0}{\kappa_f \tau} (p_f^n - p_f) , \tag{5}$$

where ρ_f^n is the fluid density in the nth set of cracks, ρ_0 is the unstressed density, κ_f is the bulk modulus of the fluid, p_f is the average (local) pressure in the fluid and τ is a relaxation parameter. Estimations of the value of τ are made by Hudson *et al.* (1996) and O'Connell & Budiansky (1977). This gives us the relationship between the fluid pressure, p_f^n, in the nth set of cracks, the average fluid pressure and the imposed static stress,

$$p_f^n = \left(p_f + i\omega\tau\kappa_f \frac{\boldsymbol{\phi}_n^1 : \boldsymbol{\sigma}^0}{\phi_n^0} \right) \Big/ (1 - i\omega\tau\gamma_n) , \tag{6}$$

with

$$\gamma_n = 1 - \frac{\kappa_f}{\kappa} + \frac{\kappa_f (\boldsymbol{\phi}_n^1)_{jj}}{\phi_n^0} , \tag{7}$$

where we have used the relationship between the fluid pressure and density,

$$\frac{\rho_0}{\rho_f^n} - 1 = -\frac{p_f^n}{\kappa_f} , \tag{8}$$

and have assumed a plane wave solution to the equations of motion of the form $\mathbf{u} = \mathbf{b}e^{i(\mathbf{k}\,.\,\mathbf{x} - \omega t)}$, so that the operators $\partial/\partial x_i$ and $\partial/\partial t$ are replaced by the factors ik_i and $-i\omega$ respectively. This is the opposite convention to that used by Hudson *et al.* (1996).

From Hudson *et al.* (1996), conservation of mass and D'Arcy's law yield an evolution equation for the total mass concentration of fluid, m_f,

$$\frac{\partial m_f}{\partial t} = \nabla . \left(\frac{\rho_f}{\eta_f} \mathbf{K}^r . \nabla p_f \right) , \tag{9}$$

with $\mathbf{K}^r$ the permeability tensor of the matrix, including cracks—in general this will be anisotropic, although Hudson *et al.* (1996) assumed an isotropic permeability; m_f is given by

$$m_f = \sum_n \rho_f^n \phi_n , \tag{10}$$

where ρ_f is the average fluid density, η_f is the fluid viscosity, and p_f and ρ_f obey the same relation as p_f^n and ρ_f^n in eq. (8).

Let us assume that $\mathbf{K}^r$ is spatially constant. Substituting eqs (4), (6) and (8) into eq. (10) and using eq. (9) we gain, to first order in p_f/κ_f and $\boldsymbol{\phi}_n^1 : \boldsymbol{\sigma}^0/\phi^0$, where ϕ^0 is the average stress-free porosity of the cracks,

$$\frac{p_f}{\kappa_f} \left[\left(1 - \frac{\kappa_f}{\kappa} \right) \sum_n \frac{\phi_n^0}{1 - i\omega\tau\gamma_n} + \kappa_f \sum_n \frac{(\boldsymbol{\phi}_n^1)_{jj}}{1 - i\omega\tau\gamma_n} + \frac{i\omega \hat{k}_p K_{pq}^r \hat{k}_q \kappa_f}{v^2 \eta_f} \right]$$
$$= -\sum_n \frac{\boldsymbol{\phi}_n^1 : \boldsymbol{\sigma}^0}{1 - i\omega\tau\gamma_n} , \tag{11}$$

where

$$\hat{k}_p = \frac{k_p}{k} \tag{12}$$

is the ratio of the wavenumber in the x_i-direction to the total wavenumber, and v is the wave speed; we approximate this to lowest order by using either v_P or v_S corresponding to P or S waves respectively.

Letting the normal to the nth set of cracks be $\mathbf{n}^n$, from Hudson *et al.* (1996) we have

$$\frac{\left(\boldsymbol{\phi}_n^1\right)_{ij}}{\phi_n^0} = \frac{2(1-\nu)}{\pi\mu\alpha_n} n_i^n n_j^n , \tag{13}$$

where $\alpha_n = c_n/a_n$ is the aspect ratio of the nth set of cracks and

$$\nu = \frac{\lambda}{2(\lambda + \mu)} \tag{14}$$

is Poisson's ratio of the matrix material. We now have

$$\gamma_n = 1 - \frac{\kappa_f}{\kappa} + \frac{2\kappa_f(1-\nu)}{\pi\mu\alpha_n} . \tag{15}$$

Substituting eq. (13) into eq. (11) yields an expression for p_f and hence by eq. (6) an expression for p_f^n in terms of $\boldsymbol{\sigma}^0$.

Thus, from eq. (4), the relative change in porosity becomes

$$\frac{\phi_n - \phi_n^0}{\phi_n^0}$$
$$= \frac{2(1-\nu)}{\pi\mu(1 - i\omega\tau\gamma_n)} \left[\frac{n_i^n n_j^n (1 - i\omega\tau)}{\alpha_n} - (\gamma_n - 1) \sum_m \frac{\varepsilon_m n_i^m n_j^m}{1 - i\omega\tau\gamma_m} \right.$$
$$\left. \times \left(\sum_m \frac{\varepsilon_m \alpha_m \gamma_m}{1 - i\omega\tau\gamma_m} + \frac{3i\omega \hat{k}_p K_{pq}^r \hat{k}_q \kappa_f}{4\pi v^2 \eta_f} \right)^{-1} \right] \sigma_{ij}^0 . \tag{16}$$

As in Hudson *et al.* (1996), we write this as

$$\frac{3}{4\pi\mu\alpha_n} N_{ij}^n \sigma_{ij}^0 , \tag{17}$$

thus defining $\{N_{ij}^n\}$, the crack opening parameters for the nth set of cracks. This is a modified version of the corresponding result derived in Hudson *et al.* (1996) that allows for variable aspect ratio.

The analysis of Hudson *et al.* (1996) now proceeds to show that the perturbation $\varepsilon\mathbf{c}^1$ in the elastic parameters is given by

$$\varepsilon c_{ipjq}^1 = -\sum_n \frac{\varepsilon_n}{\mu} l_{mk}^n n_r^n c_{krip}^0 l_{lu}^n l_{ts}^n c_{usjq}^0$$
$$\times [\delta_{t3}(\delta_{m1}\delta_{l1} + \delta_{m2}\delta_{l2}) \bar{\mathscr{U}}_{11}^n + \delta_{m3} N_{lt}^n] , \tag{18}$$

where ε_n is the crack density of the nth set of cracks; that is, $\varepsilon_n = \nu_n^s a_n^3$, where ν_n^s is the number density and a_n is the radius of the nth set of cracks.

$\{l_{ij}^n\}$ is the rotation matrix from the background axes to axes fixed in the crack with normal in the x_3-direction, so that

$$l_{3i}^n = n_i^n , \quad l_{ji}^n n_i^n = \delta_{j3} \tag{19}$$

and we have adopted the opposite convention for the definition of $\{l_{ij}^n\}$ to Hudson (1986), Hudson *et al.* (1996) and Pointer *et al.* (2000). We note that Hudson *et al.* (1996) incorrectly stated their choice of the sense of the rotation $\{l_{ij}^n\}$. The values of $\{N_{lt}^n\}$ in eq. (18) are to be calculated for cracks with normals in the x_3-direction,

$$N_{lt}^n = \frac{8}{3}\frac{(1-\nu)}{1-i\omega\tau\gamma_n}\left[\delta_{l3}\delta_{t3}(1-i\omega\tau) - \alpha_n(\gamma_n - 1) l_{li}^n l_{tj}^n \times \sum_m \frac{\varepsilon_m n_i^m n_j^m}{1-i\omega\tau\gamma_m}\left(\sum_m \frac{\varepsilon_m \alpha_m \gamma_m}{1-i\omega\tau\gamma_m} + \frac{3i\omega \hat{k}_p K_{pq}^r \hat{k}_q \kappa_{\mathrm{f}}}{4\pi v^2 \eta_{\mathrm{f}}}\right)^{-1}\right]. \tag{20}$$

$\bar{\mathscr{U}}_{11}^n$ is given by Hudson (1981) for a weak viscous material infill with effective rigidity $-i\omega\eta_{\mathrm{f}}$ as

$$\bar{\mathscr{U}}_{11}^n = \frac{16}{3}\frac{1-\nu}{2-\nu}\Big/(1+M_n), \tag{21}$$

where

$$M_n = -\frac{4i}{\pi}\frac{1-\nu}{2-\nu}\frac{\omega\eta_{\mathrm{f}}}{\mu\alpha_n}. \tag{22}$$

Inserting eq. (20) into eq. (18), we finally arrive at an expression for the first-order correction to the elastic constants,

$$\begin{aligned}\varepsilon c_{ipjq}^1 = &-\sum_n \frac{\varepsilon_n}{\mu} l_{tk}^n n_r^n c_{krip}^0 l_{lu}^n n_s^n c_{usjq}^0 \\ &\times\left[(\delta_{t1}\delta_{l1}+\delta_{t2}\delta_{l2})\bar{\mathscr{U}}_{11}^n + \frac{8}{3}\delta_{t3}\delta_{l3}(1-\nu)\frac{1-i\omega\tau}{1-i\omega\tau\gamma_n}\right] \\ &+\frac{8}{3}(1-\nu)\sum_n \frac{\varepsilon_n}{\mu} n_k^n n_r^n c_{krip}^0 c_{usjq}^0 \frac{\alpha_n(\gamma_n-1)}{1-i\omega\tau\gamma_n} \\ &\times\sum_m \frac{\varepsilon_m n_u^m n_s^m}{1-i\omega\tau\gamma_m}\left(\sum_m \frac{\varepsilon_m\alpha_m\gamma_m}{1-i\omega\tau\gamma_m} + \frac{3i\omega\hat{k}_q K_{pq}^r \hat{k}_q \kappa_{\mathrm{f}}}{4\pi v^2\eta_{\mathrm{f}}}\right)^{-1}.\end{aligned} \tag{23}$$

4 HIGH- AND LOW-FREQUENCY LIMITS

The behaviour of eq. (23) at high frequency is given by

$$\begin{aligned}\varepsilon c_{ipjq}^1 = &-\sum_n \frac{\varepsilon_n}{\mu} l_{tk}^n n_r^n c_{krip}^0 l_{lu}^n n_s^n c_{usjq}^0 \\ &\times\left[(\delta_{t1}\delta_{l1}+\delta_{t2}\delta_{l2})\bar{\mathscr{U}}_{11}^n + \frac{8}{3}\delta_{t3}\delta_{l3}(1-\nu)/\gamma_n\right],\end{aligned} \tag{24}$$

which corresponds to the result for isolated cracks filled with a fluid with $\omega\eta_{\mathrm{f}} \ll \kappa_{\mathrm{f}} \ll \kappa$ (Hudson 1981); that is, a fluid such that its effective rigidity is small in relation to its bulk modulus, which in turn is negligible in comparison with the bulk modulus of the material. The low-frequency limit of eq. (23) is

$$\begin{aligned}\varepsilon c_{ipjq}^1 = &-\frac{8}{3}(1-\nu)\sum_n \frac{\varepsilon_n}{\mu} l_{tk}^n n_r^n c_{krip}^0 l_{lu}^n n_s^n c_{usjq}^0 \\ &\times\left[(\delta_{t1}\delta_{l1}+\delta_{t2}\delta_{l2})\frac{2}{2-\nu} + \delta_{t3}\delta_{l3}\right] \\ &+\frac{8}{3}(1-\nu)\sum_n \frac{\varepsilon_n}{\mu} n_k^n n_r^n c_{krip}^0 c_{usjq}^0 \alpha_n(\gamma_n - 1) \\ &\times\sum_m \varepsilon_m n_u^m n_s^m \Big/ \sum_m \varepsilon_m\alpha_m\gamma_m,\end{aligned} \tag{25}$$

the first term of which corresponds to the result for dry cracks (Hudson 1981). However, the presence of the second term means that the response at low frequencies is that for undrained material, as we now show.

We define the compliances $\mathbf{s}$ in the same manner as we define the stiffnesses $\mathbf{c}$ (eq. 1), such that

$$\mathbf{s} = \mathbf{s}^0 + \varepsilon\mathbf{s}^1 + \mathscr{O}(\varepsilon^2), \tag{26}$$

where

$$s_{jqkr}^0 = -\frac{\lambda}{2\mu(3\lambda+2\mu)}\delta_{jq}\delta_{kr} + \frac{1}{4\mu}(\delta_{jk}\delta_{qr}+\delta_{jr}\delta_{qk}) \tag{27}$$

and

$$s_{ipjq}c_{jqkr} = c_{ipjq}s_{jqkr} = \frac{1}{2}(\delta_{ik}\delta_{pr}+\delta_{ir}\delta_{pk}). \tag{28}$$

Using the result in eq. (28) and assuming that eqs (1) and (26) represent power series, we equate the $\mathscr{O}(\varepsilon)$ terms and can therefore write $\mathbf{s}^1$ in terms of $\mathbf{c}^1$ as

$$s_{mvnw}^1 = -s_{mvip}^0 c_{ipjq}^1 s_{jqnw}^0. \tag{29}$$

Thus, for the low-frequency limit,

$$\begin{aligned}\varepsilon s_{jqkr}^1 = &\frac{8}{3}(1-\nu)\sum_n \frac{\varepsilon_n}{\mu} l_{tj}^n n_q^n l_{lk}^n n_r^n\left[(\delta_{t1}\delta_{l1}+\delta_{t2}\delta_{l2})\frac{2}{2-\nu} + \delta_{t3}\delta_{l3}\right] \\ &-\frac{8}{3}(1-\nu)\sum_n \frac{\varepsilon_n}{\mu} n_j^n n_q^n \alpha_n(\gamma_n - 1) \\ &\times\sum_m \varepsilon_m n_k^m n_r^m \Big/ \sum_m \varepsilon_m\alpha_m\gamma_m.\end{aligned} \tag{30}$$

We write

$$s_{jqkr}^1 = s_{jqkr}^{1\mathrm{a}} + s_{jqkr}^{1\mathrm{b}} \tag{31}$$

and identify $\mathbf{s}^{1\mathrm{a}}$ and $\mathbf{s}^{1\mathrm{b}}$ with the first and second terms of eq. (30) respectively. Thus, we may write the limit for dry cracks as

$$s_{jqkr}^{\mathrm{d}} = s_{jqkr}^0 + \varepsilon s_{jqkr}^{1\mathrm{a}}. \tag{32}$$

Brown & Korringa (1975) extended the work of Gassmann (1951) to give an expression for the undrained compliances in terms of the dry result,

$$s_{jqkr} = s_{jqkr}^{\mathrm{d}} + \frac{\left(s_{jqpp}^{\mathrm{d}} - s_{jqpp}^0\right)\left(s_{iikr}^{\mathrm{d}} - s_{iikr}^0\right)}{\phi^0(1/\kappa - 1/\kappa_{\mathrm{f}}) - \left(s_{llss}^{\mathrm{d}} - s_{llss}^0\right)}. \tag{33}$$

Hence, from eq. (32) and using $\phi^0 = 4\pi\varepsilon\alpha_0/3$, where $\alpha_0 = \langle\alpha\rangle$,

$$s_{jqkr} - s_{jqkr}^{\mathrm{d}} = -\frac{\varepsilon s_{jqpp}^{1\mathrm{a}} s_{iikr}^{1\mathrm{a}}}{(4\pi\alpha_0/3\kappa_{\mathrm{f}})(1-\kappa_{\mathrm{f}}/\kappa) + s_{llss}^{1\mathrm{a}}}. \tag{34}$$

From eq. (30),

$$\varepsilon s_{jqpp}^{1\mathrm{a}} = \frac{8}{3}(1-\nu)\sum_n \frac{\varepsilon_n}{\mu} n_j^n n_q^n \tag{35}$$

and

$$s_{llss}^{1\mathrm{a}} = \frac{8(1-\nu)}{3\mu}, \tag{36}$$

therefore eq. (34) becomes

$$s_{jqkr} - s^{\mathrm{d}}_{jqkr} = -\frac{8}{3}(1-\nu)\frac{2\kappa_{\mathrm{f}}(1-\nu)}{\pi\varepsilon\alpha_0\gamma_0}\sum_n \frac{\varepsilon_n}{\mu} n^n_j n^n_q \sum_m \frac{\varepsilon_m}{\mu} n^m_k n^m_r \,, \tag{37}$$

where

$$\gamma_0 = 1 - \frac{\kappa_{\mathrm{f}}}{\kappa} + \frac{2\kappa_{\mathrm{f}}(1-\nu)}{\pi\mu\alpha_0} \,. \tag{38}$$

We note that $\Sigma_m\ \varepsilon_m = \varepsilon$ and $\Sigma_m\ \varepsilon_m\alpha_m = \varepsilon\alpha_0$, provided that we assume that ε and α are independently distributed parameters; then, from the definition of γ_m (eq. 15), $\Sigma_m\ \varepsilon_m\alpha_m\gamma_m = \varepsilon\alpha_0\gamma_0$ and hence, from eq. (30),

$$\varepsilon s^{1\mathrm{b}}_{jqkr} = -\frac{8}{3}(1-\nu)\frac{\mu}{\varepsilon\alpha_0\gamma_0}\sum_n \frac{\varepsilon_n}{\mu} n^n_j n^n_q \alpha_n(\gamma_n - 1)\sum_m \frac{\varepsilon_m}{\mu} n^m_k n^m_r \,. \tag{39}$$

We can neglect the term $\kappa_{\mathrm{f}}/\kappa$ in $(\gamma_n - 1)$ on the assumption that the maximum value of the aspect ratio, $\alpha_{\max}$, satisfies the condition

$$\alpha_{\max} \ll \frac{4(1-\nu^2)}{3\pi(1-2\nu)} \,, \tag{40}$$

which is consistent with our restriction to small aspect ratios provided that $\nu \not\simeq -1$; then the term $\alpha_n(\gamma_n - 1)$ in eq. (39) is independent of n, and eq. (39) reduces to the right-hand side of eq. (37) exactly, so the undrained moduli are given by

$$s_{jqkr} = s^{\mathrm{d}}_{jqkr} - \frac{8}{3}(1-\nu)\frac{2\kappa_{\mathrm{f}}(1-\nu)}{\pi\varepsilon\alpha_0\gamma_0}\sum_n \frac{\varepsilon_n}{\mu} n^n_j n^n_q \sum_m \frac{\varepsilon_m}{\mu} n^m_k n^m_r \,. \tag{41}$$

This is identical to eq. (30) for the low-frequency limit for connected cracks, showing that, at low frequencies, connected cracks respond at each point in exactly the same way as the same material under static, undrained conditions.

5 CONTINUOUS LIMIT

Having developed the theory from a discrete perspective, we shall henceforth assume a continuous limit: $\Sigma_n\ F(n)$ in eq. (23) is replaced by

$$\int_{\alpha=0}^{\infty}\int_{a=0}^{\infty}\int_{\theta=0}^{\pi}\int_{\phi=0}^{2\pi} F(\phi,\theta,a,\alpha) f_\alpha f_a f_{\mathbf{n}} \sin\theta\, d\phi\, d\theta\, da\, d\alpha \tag{42}$$

for any function F, where f_α, f_a and $f_{\mathbf{n}}$ are the probability distribution functions of the random variables α, a and $\mathbf{n}$ (defined by polar angles ϕ and θ) respectively. We shall assume that these distributions are independent of one another, for the purpose of separately assessing their effects on seismic anisotropy. More realistically perhaps, one would expect aspect ratio to depend upon orientation, with cracks parallel to the direction of maximum principal stress having a larger mean aspect ratio than those perpendicular to it. Gibson & Toksöz (1990) developed a model of a probability density function for crack orientation with an aspect ratio distribution included. Their results from the inversion of velocity measurements are generally good, although there is an implied non-uniqueness of inversion.

Prior to the exposure to stress, a rock will have a generally isotropic background distribution of cracks (David *et al.* 1999). Stress will induce further cracking, which will be of an anisotropic nature (Menéndez *et al.* 1999), and thus a more accurate description of crack distributions within a rock may be obtained by representing the crack distribution as the sum of an isotropic and an anisotropic part.

For a given aspect ratio, the crack radius a_n only appears within the term ε_n in eq. (23), so that in the continuous limit it occurs in the form of $\langle a^3\rangle$ only, and thus ε_n may be replaced everywhere by ε.

6 ALIGNED CRACKS

If we take the limit in which the cracks are fully aligned and of identical aspect ratio, we find that $\mathbf{c}^1$ is given by eq. (3), with

$$\bar{\mathscr{U}}_{11} = \frac{16}{3}\frac{1-\nu}{2-\nu}\Big/\left(1 + M^{\mathrm{align}}\right), \tag{43}$$

$$\bar{\mathscr{U}}_{33} = \frac{8}{3}(1-\nu)/(1 + K^{\mathrm{align}}) \tag{44}$$

and

$$M^{\mathrm{align}} = -\frac{4i}{\pi}\frac{1-\nu}{2-\nu}\,\omega\tau P^m \,, \tag{45}$$

$$K^{\mathrm{align}} = \left(\frac{2\kappa_{\mathrm{f}}(1-\nu)}{\pi\mu\alpha_0} - \frac{\kappa_{\mathrm{f}}}{\kappa}\right)\left(1 + \frac{i\omega\tau P^k}{1 + (\omega\tau)^2 P^k}\right)^{-1} , \tag{46}$$

where

$$P^m = \frac{\eta_{\mathrm{f}}}{\mu\alpha_0\tau} \tag{47}$$

and

$$P^k = \frac{3\kappa_{\mathrm{f}}\hat{k}_p K^r_{pq}\hat{k}_q}{4\pi\varepsilon\alpha_0 v^2\tau\eta_{\mathrm{f}}} \,. \tag{48}$$

The quantity $\omega\tau P^m$ is identical to the intracrack viscosity parameter P_v of Pointer *et al.* (2000), who estimated that, with the fluid properties of oil or water, its effect is negligible for seismological applications for both aligned and randomly oriented cracks.

We have written the expressions in eqs (45) and (46) in terms of $\omega\tau$, which is the short-range diffusion parameter P_{srd} of Pointer *et al.* (2000) and the quantity $\omega\tau P^k$ is $3/4\pi$ times the long-range diffusion parameter P_{lrd} of Pointer *et al.* (2000). Apart from the presence of an additional term—the $\kappa_{\mathrm{f}}/\kappa$ term, neglected by Hudson *et al.* (1996)—this result is identical to the aligned limit of the expression derived for non-aligned cracks by Hudson *et al.* (1996). Both of these expressions for aligned cracks with identical aspect ratio differ from that given by Hudson *et al.* (1996) in the value of the parameter K^{align}; the formula given by Hudson *et al.* (1996) is

$$K^{\mathrm{align}} = \frac{2\kappa_{\mathrm{f}}(1-\nu)}{\pi\mu\alpha_0}\left(1 - i\omega\tau P^k\right)^{-1} , \tag{49}$$

which ignores the term $(\omega\tau)^2 P^k$ and uses the opposite sign convention on the temporal derivative. This difference arises as a result of the failure of the aligned cracks result (Hudson *et al.* 1996) to account for any local fluid flow (note that $\omega\tau P^k$ is independent of τ).

We see from eq. (46) that in either of the limits $\omega\tau\to 0$ or $\omega\tau\to\infty$,

$$K^{\mathrm{align}}\to\frac{2\kappa_{\mathrm{f}}(1-\nu)}{\pi\mu\alpha_0}-\frac{\kappa_{\mathrm{f}}}{\kappa}\,, \tag{50}$$

which is the result for isolated cracks filled with a fluid with $\omega n_{\mathrm{f}}\ll\kappa_{\mathrm{f}}\ll\kappa$ (Hudson 1981). The inclusion of local crack-to-crack flow gives the expected result at high frequencies, but at very low frequencies the cracks still act as if isolated for the reasons given earlier.

7 VARIABLE ASPECT RATIO

To begin with, we assume that the cracks are fully aligned, hence

$$f_{\mathbf{n}}(\theta,\phi|\theta_0,\phi_0)=\delta(\theta-\theta_0)\delta(\phi-\phi_0)/\sin\theta\,, \tag{51}$$

and consider the effects of variable aspect ratio only. Let us further assume that $\theta_0=0$, so that all the cracks now have normals in the x_3-direction. Eq. (23) now takes a form identical to that of eq. (3),

$$c^1_{ipjq}=-\frac{1}{\mu}\,c^0_{k3ip}c^0_{l3jq}\tilde{\mathscr{U}}_{kl}\,, \tag{52}$$

where $\{\tilde{\mathscr{U}}_{ij}\}$ is a diagonal matrix with

$$\tilde{\mathscr{U}}_{11}=\tilde{\mathscr{U}}_{22}=\frac{16}{3}\frac{1-\nu}{2-\nu}\Big/(1+M')\,, \tag{53}$$

$$\tilde{\mathscr{U}}_{33}=\frac{8}{3}\,(1-\nu)F_1/(1+K') \tag{54}$$

and

$$M'=-\frac{4i}{\pi}\frac{1-\nu}{2-\nu}\,\omega\tau P^m E(m)\left[1+\frac{4i}{\pi}\frac{1-\nu}{2-\nu}\,\omega\tau P^m E(m)\right]^{-1}, \tag{55}$$

$$K'=(\gamma_0-1)\times\left[1+\frac{i\omega\tau P^k+(F_2-F_1)\frac{1+(\kappa_{\mathrm{f}}/\kappa)(\gamma_0-1)^{-1}}{1-i\omega\tau\gamma_0}}{F_1-(F_2-F_1)\frac{i\omega\tau(1-\kappa_{\mathrm{f}}/\kappa)+(\kappa_{\mathrm{f}}/\kappa)(\gamma_0-1)^{-1}}{1-i\omega\tau\gamma_0}+(\omega\tau)^2P^k}\right]^{-1}. \tag{56}$$

We have defined here two functions that depend upon the probability distribution function of α,

$$F_1\equiv(1-i\omega\tau\gamma_0)\int_0^\infty\frac{f_\alpha d\alpha}{1-i\omega\tau\gamma}=\frac{1-i\omega\tau\gamma_0}{(1-i\omega\tau(1-\kappa_{\mathrm{f}}/\kappa))^2}\times\left[1-i\omega\tau\Big(1-\frac{\kappa_{\mathrm{f}}}{\kappa}\Big)+i\omega\tau\Big(\gamma_0-1+\frac{\kappa_{\mathrm{f}}}{\kappa}\Big)E(k)\right] \tag{57}$$

and

$$\begin{aligned}F_2&\equiv\frac{1-i\omega\tau\gamma_0}{\alpha_0}\int_0^\infty\frac{\alpha f_\alpha d\alpha}{1-i\omega\tau\gamma}\\&=\frac{1-i\omega\tau\gamma_0}{(1-i\omega\tau(1-\kappa_{\mathrm{f}}/\kappa))^3}\left[\left(1-i\omega\tau\Big(\frac{1-\kappa_{\mathrm{f}}}{\kappa}\Big)\right)^2\right.\\&\quad+i\omega\tau\Big(\gamma_0-1+\frac{\kappa_{\mathrm{f}}}{\kappa}\Big)\Big(1-i\omega\tau\Big(1-\frac{\kappa_{\mathrm{f}}}{\kappa}\Big)\Big)\\&\quad\left.-(\omega\tau)^2\Big(\gamma_0-1+\frac{\kappa_{\mathrm{f}}}{\kappa}\Big)^2E(k)\right],\end{aligned} \tag{58}$$

where

$$E(y)=\alpha_0\left\langle\frac{1}{\alpha+\alpha_0 y}\right\rangle, \tag{59}$$

and the parameters of the distribution are chosen such that $\langle\alpha\rangle=\alpha_0$. Finally,

$$k=-\frac{2\kappa_{\mathrm{f}}(1-\nu)}{\pi\mu\alpha_0}\,\frac{i\omega\tau}{1-i\omega\tau(1-\kappa_{\mathrm{f}}/\kappa)} \tag{60}$$

and

$$m=-\frac{4i}{\pi}\frac{1-\nu}{2-\nu}\,\omega\tau P^m\,. \tag{61}$$

We can generalize this result to the case of arbitrary values of θ_0 and ϕ_0, letting the normal to the cracks be $\mathbf{n}^0=(\sin\theta_0\cos\phi_0,\sin\theta_0\sin\phi_0,\cos\theta_0)^{\mathrm{T}}$,

$$c^1_{ipjq}=-\frac{1}{\mu}\,n^0_r c^0_{krip}n^0_s c^0_{lsjq}\tilde{U}_{kl}\,, \tag{62}$$

where $\{\tilde{U}_{ij}\}$ is just the rotation of $\{\tilde{\mathscr{U}}_{ij}\}$ to the new axes and is given by

$$\tilde{U}_{ij}=\left(\delta_{ij}-n^0_in^0_j\right)\tilde{\mathscr{U}}_{11}+n^0_in^0_j\tilde{\mathscr{U}}_{33}\,, \tag{63}$$

with $\tilde{\mathscr{U}}_{11}$ and $\tilde{\mathscr{U}}_{33}$ given as above (eqs 53 and 54).

7.1 Modelling the distribution

Our theory restricts us to consider $\alpha\ll 1$ only, so we look for distributions with a finite range and a small mean. For this we have chosen a generalized form of the Beta distribution (e.g. Ross 1989), Beta(u, p, q), with a probability density function (pdf)

$$f_\alpha(\alpha|u,p,q)=\frac{1}{u\mathrm{B}(p,q)}\Big(\frac{\alpha}{u}\Big)^{p-1}\Big(1-\frac{\alpha}{u}\Big)^{q-1}\quad\text{for}\quad 0\le\alpha\le u,\quad\text{with}\quad p,q>0\,, \tag{64}$$

and $\mathrm{B}(x, y)$ is the Beta function (e.g. Carrier *et al.* 1983). The three parameters p, q and u allow us considerable flexibility with our model and in particular we may choose them such that the pdf closely resembles observational results (Hay *et al.* 1988).

We wish to fit the parameters of the distribution such that

$$\begin{aligned}&\langle\alpha\rangle=\alpha_0\,,\\&\mathrm{Var}(\alpha)\equiv\langle\alpha^2\rangle-\langle\alpha\rangle^2=(\delta\alpha_0)^2\,,\end{aligned} \tag{65}$$

for some δ. Thus we choose p and q such that

$$\begin{aligned}p&=\frac{u-\alpha_0-\alpha_0\delta^2}{u\delta^2}\,,\\q&=\frac{u-\alpha_0}{\alpha_0}\,p\,.\end{aligned} \tag{66}$$

Our choice of δ will dictate the spread of the distribution and $u=\alpha_{\max}$, the maximum value of α that can be achieved.

Choosing $u=0.2$, $\alpha_0=0.00837$ and $\delta=0.703$ ensures that our probability density function resembles the results of Hay *et al.* (1988) (see Fig. 2) based upon a truncation of the data provided in Hay (1988), where the larger aspect ratio values have been ignored. For α greater than some critical value much less than u, the pdf is effectively zero; it is not surprising, therefore, that variations in u have a negligible effect upon the

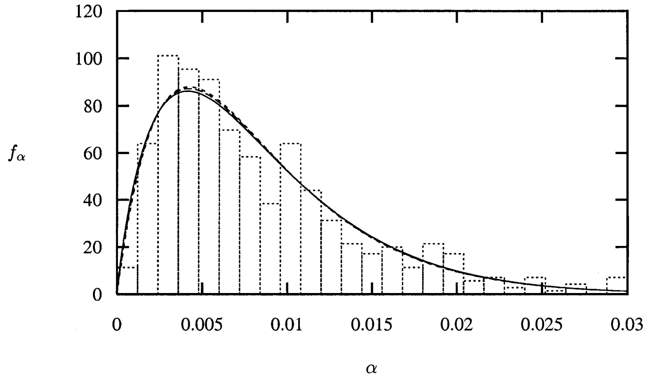

Figure 2. The generalized Beta distribution, with mean $\alpha_0=0.00837$, variance governed by $\delta=0.703$ and width $u=0.2$ (solid line), $u=0.5$ (long dashes), and the Gamma distribution governed by the same values of α_0 and δ (medium dashes) to approximate the sum of the crack aspect ratio observations for grain boundary, intergranular and intragranular cracks of Hay *et al.* (1988) (bars).

values of the elastic constants—while there is a very small observable difference between the Beta distribution with $u=0.2$ and 0.5 (Fig. 2), there is no discernible difference between the resulting components of the stiffnesses (eq. 52)—so we replace eq. (64) with

$$f_\alpha(\alpha|\alpha_0,\delta) = \lim_{u\to\infty} f_\alpha(\alpha|u,p,q)$$

$$= \frac{\left(\alpha_0\delta^2\right)^{-1/\delta^2}}{\Gamma\left(1/\delta^2\right)}\,\alpha^{1/\delta^2-1}\,\mathrm{e}^{-\alpha/\alpha_0\delta^2}, \quad \text{for} \quad 0\le\alpha, \tag{67}$$

which is a Gamma($1/\delta^2$, $1/\alpha_0\delta^2$) distribution (Ross 1989), with $\Gamma(z)$ the Gamma function (Carrier *et al.* 1983). Graphically, this looks almost identical to the Beta distribution with $u=0.5$ (Fig. 2). With this choice of distribution, we have

$$E(y) = \frac{1/\delta^2}{\Gamma\left(1/\delta^2\right)}\int_0^\infty \frac{x^{1/\delta^2-1}\,\mathrm{e}^{-x}}{x+y/\delta^2}\,dx\,. \tag{68}$$

7.2 Results

We start by choosing the parameters of the Gamma distribution such that it closely follows the measurements of Hay *et al.* (1988); thus $\alpha_0=0.00837$ and $\delta=0.703$. Furthermore, we shall use $\varepsilon=0.02$, $v_P=3.5\times10^3$ m s^{-1}, $v_S=2.0\times10^3$ m s^{-1} and $\rho=2.2\times10^3$ kg m^{-3} (average values that could correspond to a large number of possible matrix materials), $\kappa_\mathrm{f}=2.25\times10^9$ Pa and $\eta_\mathrm{f}=10^{-3}$ Pa s (for water), thus $v=0.258$ and $\kappa_\mathrm{f}/\kappa=0.148$. We shall, for simplicity, assume that $\{K^r_{pq}\}=K^r\delta_{pq}$ and use $K^r=10^3$ mD ($\simeq10^{-12}$ m^2), so that only the parameter τ remains unknown in the expressions for P^m and P^k (eqs 47 and 48 respectively).

We start by considering the variation of Thomsen's parameters (see Appendix B) with the non-dimensional frequency $\omega\tau$ and the constants P^k and P^m. From the definitions (eqs B1, B2 and B3),

$$\varepsilon_T = \frac{4\varepsilon v}{1-2v}\,\mathscr{Re}\left(\tilde{\mathscr{U}}_{33}\right), \tag{69}$$

$$\delta_T = \varepsilon\left[2\mathscr{Re}\left(\tilde{\mathscr{U}}_{33}\right) - \frac{1-2v}{1-v}\,\mathscr{Re}\left(\tilde{\mathscr{U}}_{11}\right)\right] \tag{70}$$

and

$$\gamma_T = \frac{\varepsilon}{2}\,\mathscr{Re}\left(\tilde{\mathscr{U}}_{11}\right) \tag{71}$$

to first order in crack density ε. Thus ε_T (a measure of the P-wave anisotropy) is independent of P^m and, from Fig. 3(a), is described by a bell-shaped curve for lower values of P^k that develops a flat top for higher values, while γ_T (a measure of the SH-wave anisotropy) is independent of P^k and is described by a monotonically decreasing curve (see Fig. 3b); δ_T depends upon both P^k and P^m.

We see from Fig. 3(a) that increasing P^k results in an increase in the magnitude of the peak of ε_T up to a maximum reached at $P^k\simeq10^6$ and a decrease in the value of $\omega\tau$ at which the peak occurs, at approximately $\omega\tau=(P^k)^{-1/2}$—thus we see that the term $(\omega\tau)^2P^k$ dominates eq. (56). Increasing P^k still further does not change the peak value of ε_T, but broadens the range of $\omega\tau$ within which ε_T is non-negligible.

From Fig. 3(b) it can be seen that an order of magnitude increase in the value of P^m results in an order of magnitude decrease in the value of $\omega\tau$ at which a transition is made from

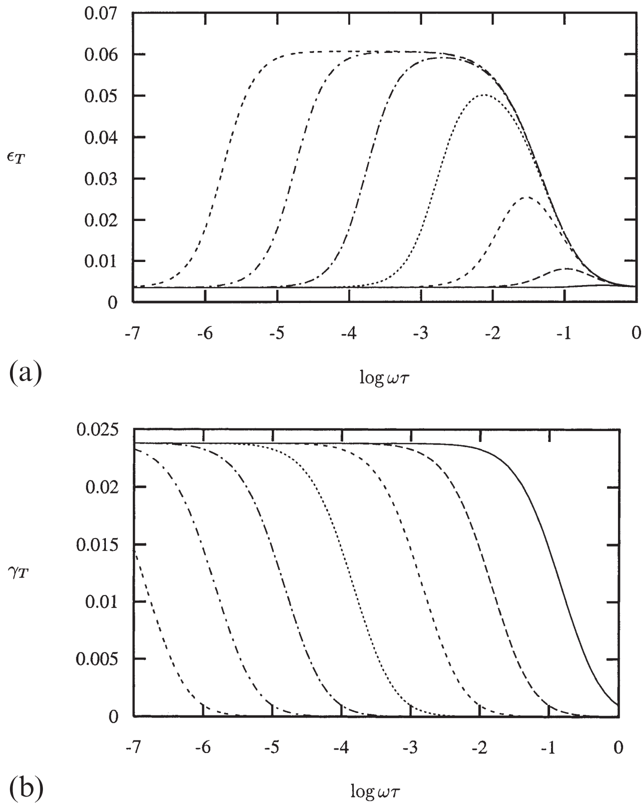

Figure 3. (a) Thomsen's parameter ε_T as a function of non-dimensional frequency $\omega\tau$ for $P^k=10$ (solid line), 10^2 (long dashes), 10^3 (medium dashes), 10^4 (short dashes), 10^5 (long dash-dot), 10^6 (short dash-dot) and 10^7 (double dashes), with the Gamma distribution given in Fig. 2 for the aspect ratio and crack density $\varepsilon=0.02$. (b) Thomsen's parameter γ_T as a function of non-dimensional frequency $\omega\tau$ for $P^m=10$ (solid line), 10^2 (long dashes), 10^3 (medium dashes), 10^4 (short dashes), 10^5 (long dash-dot), 10^6 (short dash-dot) and 10^7 (double dashes), with the Gamma distribution given in Fig. 2 for the aspect ratio and crack density $\varepsilon=0.02$.

the maximum to the minimum values of γ_T (as $\omega\tau \rightarrow \infty$, $E_m \rightarrow 0$ such that $M' \rightarrow \infty$ and thus $\tilde{\mathscr{U}}_{11} \rightarrow 0$) with the transition occurring over a range $[0.1\ (P^m)^{-1}, 10\ (P^m)^{-1}]$ of $\omega\tau$.

We now consider the effect upon Thomsen's parameters of the distribution parameter δ and the crack density ε. In Fig. 4(a) we consider the effect of δ and ε upon ε_T, for $P^k = 10^4$. We see that a decrease in the variance of the distribution increases the value of ε_T at its peak—that is, it increases the degree of anisotropy, as we would expect. The greatest value of

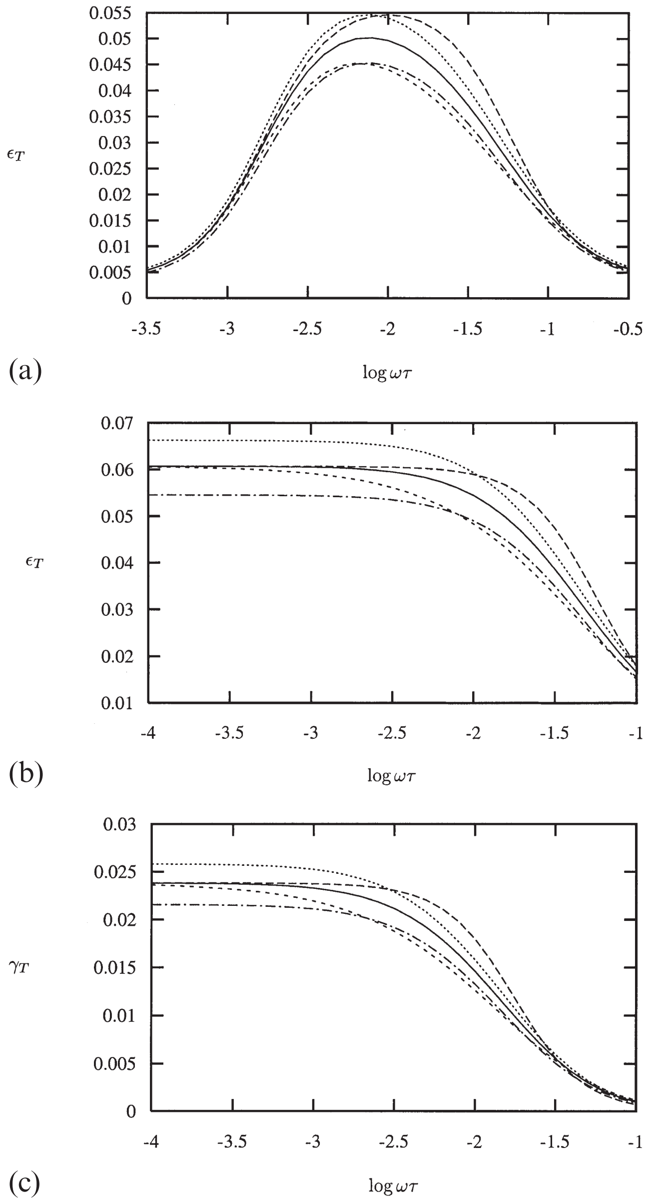

Figure 4. (a) Thomsen's parameter ε_T as a function of non-dimensional frequency $\omega\tau$ for $P^k = 10^4$, with distribution parameter $\delta = 0.703$ (solid line), 0 (long dashes) and 1.0 (medium dashes), and crack density $\varepsilon = 0.02$, also with $\delta = 0.703$, $\varepsilon = 0.0216$ (short dashes) and 0.0182 (long dash-dot). (b) As (a), but with $P^k = 10^8$. (c) Thomsen's parameter γ_T as a function of non-dimensional frequency $\omega\tau$ for $P^m = 10^2$, with distribution parameter $\delta = 0.703$ (solid line), 0 (long dashes) and 1.0 (medium dashes), and crack density $\varepsilon = 0.02$, also with $\delta = 0.703$, $\varepsilon = 0.0216$ (short dashes) and 0.0182 (long dash-dot).

ε_T is obtained for $\delta = 0$, where all the cracks have the same aspect ratio. Although this case corresponds to an anomalous result for the elastic moduli at low frequencies, we see that the behaviour of ε_T in the limit $\delta \rightarrow 0$ is not remarkable. Away from the peak value, little change is seen in the value of ε_T when δ is varied. Furthermore, we note that an increase in the crack density also serves to increase the peak value of ε_T—thus decreasing the variance from 0.703 to 0 (the aligned case) produces a result that is very similar to that achieved by increasing the crack density from 0.2 to 0.0216, and similarly, increasing the variance to 1.0 (an exponential distribution) is seen to be almost equivalent to decreasing the crack density to 0.0182.

So can we distinguish between the effects of the crack density ε and the variance of the aspect ratio distribution δ? At values of $\omega\tau$ away from the peak value of ε_T, a change in δ will not affect the value of ε_T, whereas an increase or decrease in ε will cause an increase or decrease, respectively, in ε_T; however, this effect is barely discernible for such small changes in ε as those discussed above. For larger values of P^k, we are more able to distinguish between the two effects (see Fig. 4b), where now $P^k = 10^8$. Only a small change is seen in ε_T with δ, but a notably different change is seen when adjusting the value of ε.

Fig. 4(c) shows how γ_T varies with δ and ε, for $P^m = 10^2$. We see that a reduction in the variance of the aspect ratio distribution will increase the value of $\omega\tau$ at which the transition from the maximum to minimum values of γ_T begins, without affecting the point at which the minimum value is reached. This effect can be distinguished from changes in the value of ε, which clearly increases or decreases the maximum value of γ_T with $\omega\tau$ as it is increased or decreased respectively.

The attenuation coefficients Q^{-1} for the three waves are defined in eqs (C13), (C14) and (C15); these are dependent upon the incident angle of a wave. For an incident wave parallel to the direction of the crack normals (and thus perpendicular to the cracks), the x_3-direction, the change in Q^{-1}_{qP} with frequency is shown in Fig. 5(a) for different values of the parameter P^k and Fig. 5(b) for different values of ε and δ. For values of P^k smaller than about 10^3 there is a single peak in the value of Q^{-1}_{qP}. For sufficiently large P^k this peak remains at a fixed frequency and amplitude, while a second peak occurs at a frequency that decreases as P^k increases. Comparing Figs 3(a) and 5(a), we see that the frequencies at which the peaks in the attenuation parameter Q^{-1}_{qP} occur coincide with the frequencies of the maximum gradient in the corresponding plot of ε_T. A change in ε clearly changes the magnitude of both peaks (see Fig. 5b) and a change in δ produces a larger change in the magnitude of the higher-frequency peak than it does in the lower-frequency peak. Indeed, for larger values of P^k, a change in δ has no effect on the magnitude of the low-frequency peak. Thus, we can always adjust the value of ε to mimic the effect on the high-frequency peak in Q^{-1}_{qP} of a change in δ, but both peaks cannot be simultaneously matched. The relative heights of the two peaks should be able to give us an indication of the value of δ, assuming that both frequencies are seismically possible. At an incident angle parallel to the cracks, Q^{-1}_{qP} shows a similar variation with the parameters P^k, ε and δ, but is of an order of magnitude smaller (not shown).

Being able to distinguish between the effects of δ and ε on Q^{-1}_{qSH} is far less likely (see Fig. 6). The frequency at which the peak in Q^{-1}_{qSH} occurs coincides with the frequency at which the corresponding plot of γ_T has a maximum gradient (see Fig. 3b).

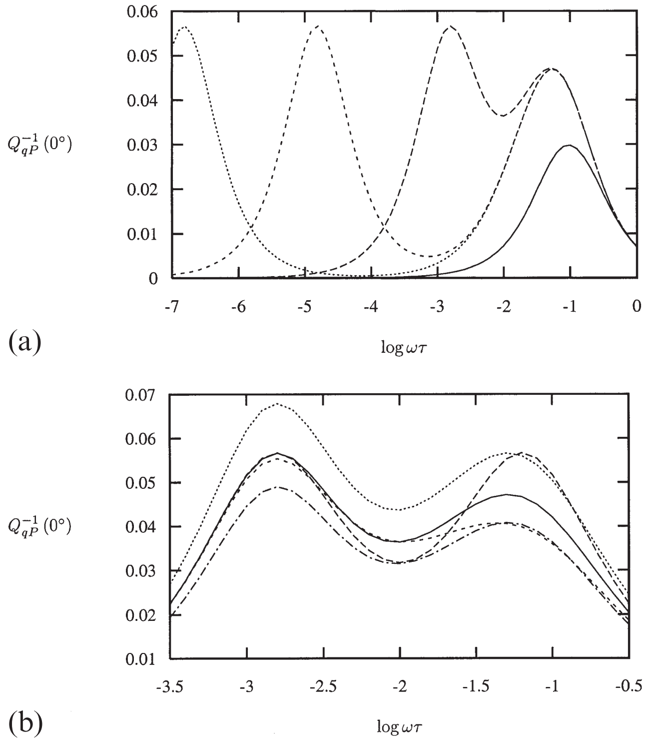

Figure 5. (a) The *P*-wave attenuation parameter Q_{qP}^{-1} for an incident wave perpendicular to the cracks as a function of non-dimensional frequency $\omega\tau$ for $P^k = 10^2$ (solid line), 10^4 (long dashes), 10^6 (medium dashes) and 10^8 (short dashes), with $\varepsilon = 0.02$ and the Gamma distribution given in Fig. 2 for the aspect ratio. (b) The *P*-wave attenuation parameter Q_{qP}^{-1} for an incident wave perpendicular to the cracks as a function of non-dimensional frequency $\omega\tau$ for $P^k = 10^4$, with distribution parameter $\delta = 0.703$ (solid line), 0 (long dashes) and 1.0 (medium dashes), and crack density $\varepsilon = 0.02$, also with $\delta = 0.703$, $\varepsilon = 0.024$ (short dashes) and 0.0173 (long dash-dot).

8 VARIABLE ORIENTATION

We shall now consider the effects of allowing the orientation of the crack normals to vary while keeping α constant; thus

$$f_\alpha(\alpha|\alpha_0) = \delta(\alpha - \alpha_0)\,. \tag{72}$$

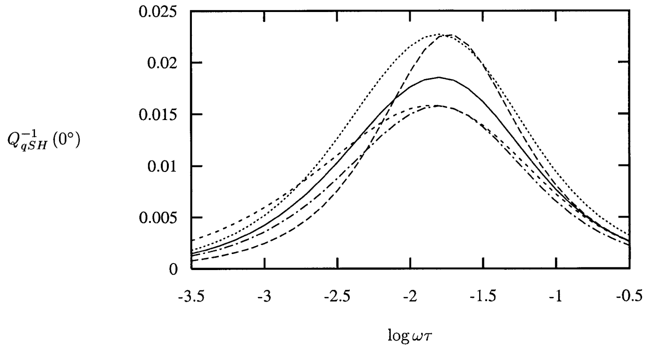

Figure 6. The *SH*-wave attenuation parameter Q_{qSH}^{-1} for an incident wave perpendicular to the cracks as a function of non-dimensional frequency $\omega\tau$ for $P^m = 10^2$, with distribution parameter $\delta = 0.703$ (solid line), 0 (long dashes) and 1.0 (medium dashes), and crack density $\varepsilon = 0.02$, also with $\delta = 0.703$, $\varepsilon = 0.0245$ (short dashes) and 0.017 (long dash-dot).

We find that

$$c^1_{ipjq} = -\frac{1}{\mu}\, c^0_{krip} c^0_{usjq} T_{krus}\,, \tag{73}$$

where

$$T_{krus} = \left[(\delta_{t1}\delta_{l1} + \delta_{t2}\delta_{l2})\bar{\mathscr{U}}_{11} + \frac{8}{3}\,\delta_{t3}\delta_{l3}(1-\nu)\,\frac{1 - i\omega\tau}{1 - i\omega\tau\gamma_0}\right]\Omega_{tkrlus} - \frac{8}{3}\,(1-\nu)\,\frac{\gamma_0 - 1}{1 - i\omega\tau\gamma_0}\,\Pi_{kr}\Pi_{us}[\gamma_0 + i\omega\tau P^k(1 - i\omega\tau\gamma_0)]^{-1}\,, \tag{74}$$

$$\Omega_{tkrlus} = \int_{\theta=0}^{\pi}\int_{\phi=0}^{2\pi} l_{tk} n_r l_{lu} n_s f_{\mathbf{n}} \sin\theta\, d\phi\, d\theta \tag{75}$$

and

$$\Pi_{kr} = \int_{\theta=0}^{\pi}\int_{\phi=0}^{2\pi} n_k n_r f_{\mathbf{n}} \sin\theta\, d\phi\, d\theta\,. \tag{76}$$

$\bar{\mathscr{U}}_{11}$ is given by

$$\bar{\mathscr{U}}_{11} = \frac{16}{3}\,\frac{1-\nu}{2-\nu}\Big/(1 + M)\,, \tag{77}$$

$$M = -\frac{4i}{\pi}\,\frac{1-\nu}{2-\nu}\,\omega\tau P^m\,. \tag{78}$$

8.1 Modelling the distribution

We shall make the assumption that the crack distribution is rotationally symmetric—that is, the cracks are uniformly distributed with respect to ϕ—and consider distributions for $\mathbf{n}$ that are concentrated around a mean orientation. We use the Watson distribution (Mardia 1972; Fisher *et al.* 1987), a bipolar distribution, such that

$$f_{\mathbf{n}} = \frac{b(k)}{2\pi}\, e^{k(\sin\theta\sin\theta_0\cos(\phi-\phi_0) + \cos\theta\cos\theta_0)^2} \quad \text{for} \quad 0 \le \theta \le \pi/2,\ 0 \le \phi \le 2\pi \text{ and } k \ge 0\,, \tag{79}$$

where

$$b(k) = 1\Big/\left(\int_0^1 e^{kt^2}\, dt\right) \tag{80}$$

and we have restricted the range of θ to half that given in the original definition of the distribution, to avoid any ambiguity in the definition of crack-normal orientation (as Peacock & Hudson 1990). We shall take $\theta_0 = 0$ so that the mean orientation of the normal, $\mathbf{n}^0 = (0, 0, 1)^{\mathrm{T}}$, is along the x_3-axis, and the resulting effective medium is vertically transversely isotropic.

The parameter k is a measure of the variance of the distribution,

$$\mathrm{Var}(\mathbf{n}) \equiv \left\langle \left|\mathbf{n} - \mathbf{n}^0\right|^2 \right\rangle = 2 - 2I_{1,1}\,, \tag{81}$$

where the integral $I_{m,n}$ is defined by eq. (D1). $k = 0$ corresponds to a uniform (isotropic) distribution and as $k \to \infty$ the distribution approaches a delta-like function (eq. 51), so that the cracks are fully aligned. With this distribution, we find that

$\{\Pi_{kr}\}$ is diagonal, with

$$\Pi_{11} = \Pi_{22} = \frac{1}{2} I_{3,0}\,, \qquad \Pi_{33} = I_{1,2}\,. \tag{82}$$

To evaluate the components of $\{\Omega_{tkrlus}\}$ we must find $\{l_{ij}\}$, given that

$$l_{3i} = n_i\,, \quad l_{ji} n_i = \delta_{j3}\,. \tag{83}$$

The rotation $\{l_{ij}\}$ is given by Fisher *et al.* (1987) as

$$\{l_{ij}\} = \begin{pmatrix} \cos\theta\cos\phi\cos\psi - \sin\phi\sin\psi & \cos\theta\sin\phi\cos\psi + \cos\phi\sin\psi & -\sin\theta\cos\psi \\ -\cos\theta\cos\phi\sin\psi - \sin\phi\cos\psi & -\cos\theta\sin\phi\sin\psi + \cos\phi\cos\psi & \sin\theta\sin\psi \\ \sin\theta\cos\phi & \sin\theta\sin\phi & \cos\theta \end{pmatrix}, \tag{84}$$

where ψ represents an arbitrary rotation about the x_3-axis. $\{T_{krus}\}$ (eq. 74) is independent of the angle ψ, and those elements of $\{\Omega_{tkrlus}\}$ that contribute to $\{T_{krus}\}$ are given in Appendix D.

8.2 Results

The effect upon Thomsen's parameters of the crack orientation distribution is now considered. We examine how they vary with $\omega\tau$, P^k, P^m, ε and the distribution parameter k. We use the same values of all of the parameters as with the variable aspect ratio model.

We no longer have such simple expressions for Thomsen's parameters as eqs (69), (70) and (71), while γ_T remains independent of the parameter P^k, and ε_T now depends upon both P^k and P^m, as does δ_T, as before. When $k=0.0$, the distribution of crack-normal orientations is uniform (i.e. isotropic) and all of Thomsen's parameters are identically zero. For $k=10.0$, the distribution of crack-normal orientations about the mean is given in Fig. 7, and with $P^m=10^4$, the variation of ε_T with $\omega\tau$ for a range of values of P^k is shown in Fig. 8(a). We note that Figs 8(a) and 3(a) look very similar; however, it is not now until $P_k=10^7$ that ε_T reaches its largest peak value. The peak values obtained are less than the corresponding ones in Fig. 3(a).

By choosing a different value of P^m, we would have made only a minimal difference to Fig. 8(a). A smaller value of P^m would result in a larger value for ε_T, but only for smaller values of P^k, whereas a larger value of P^m would reduce ε_T for the larger values of P^k—these effects would be difficult to distinguish from either a larger value of the distribution parameter k or a more tightly concentrated distribution or an increased crack density ε.

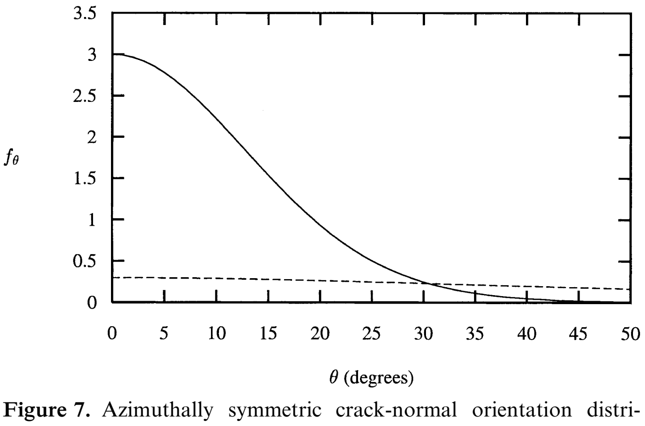

Figure 7. Azimuthally symmetric crack-normal orientation distribution with variance governed by the parameter $k=10.0$ (solid line) and $k=1.0$ (long dashes).

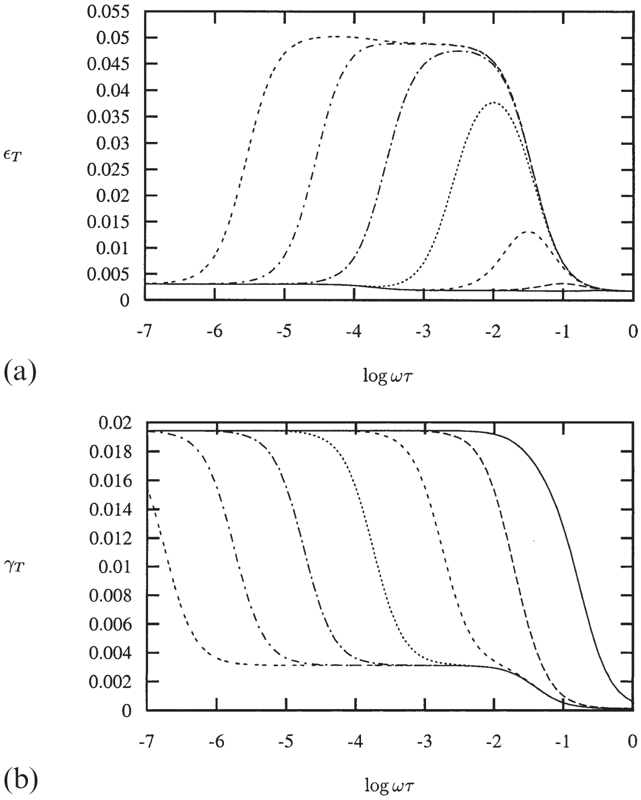

Figure 8. (a) Thomsen's parameter ε_T as a function of non-dimensional frequency $\omega\tau$ with $P^m=10^4$ and the same values of P^k as in Fig. 3(a) with orientation distribution as in Fig. 7. (b) Thomsen's parameter γ_T as a function of non-dimensional frequency $\omega\tau$ with the same values of P^m as in Fig. 3(b) and distribution as in Fig. 7.

In Fig. 8(b) we show the variation of γ_T with P^m (independent of P^k); compare this with Fig. 3(b). Certainly there is a considerable similarity, as with ε_T; however, for $P^m=10^4$ and higher, the transition from the maximal to minimal values of γ_T occurs over a larger range of $\omega\tau$ than for the variable aspect ratio model; indeed, for P^m higher than 10^4, γ_T appears to reach a non-zero minimal value before finally approaching zero at higher values of $\omega\tau$.

For the choice of parameters $P^k=10^4$ and $P^m=10^4$, the effect on ε_T of a change in k is indistinguishable from a change in ε, except perhaps at low frequencies. From Fig. 9(a) it is seen that increasing k to infinity (the fully aligned limit) appears identical to increasing the crack density to $\varepsilon=0.0242$, while decreasing k to 1.0 appears indistinguishable from decreasing ε to 0.0034. Altering the value of P^k or P^m does not increase the difference between the effect on ε_T of changes in k and ε.

For a smaller value of k, the difference between Figs 8(b) and 3(b) is amplified, while for a larger value of k, Fig. 8(b) becomes indistinguishable from Fig. 3(b)—compare the long dashed lines in Figs 4(c) and 9(b). This is as we would expect, that a very small perturbation in either the crack-normal or aspect ratio distributions from the perfectly aligned identical aspect ratio limit would be indistinguishable.

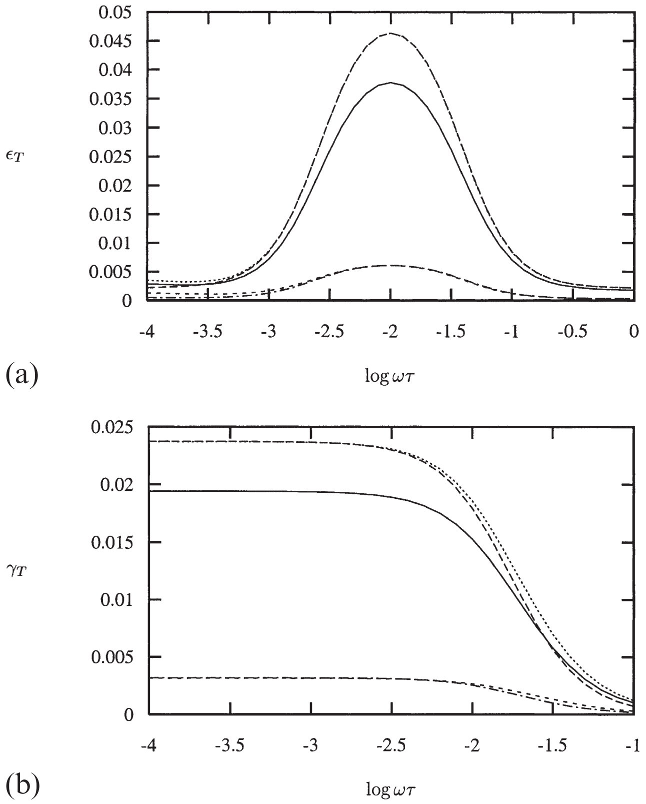

Figure 9. (a) Thomsen's parameter ε_T as a function of non-dimensional frequency $\omega\tau$ for $P^k = 10^4$ and $P^m = 10^4$, with distribution parameter $k = 10.0$ (solid line), ∞ (long dashes) and 1.0 (medium dashes), and crack density $\varepsilon = 0.02$, also with $k = 10.0$, $\varepsilon = 0.0242$ (short dashes) and 0.0034 (long dash-dot). (b) Thomsen's parameter γ_T as a function of non-dimensional frequency $\omega\tau$ for $P^m = 10^2$ with distribution parameter $k = 10.0$ (solid line), ∞ (long dashes) and 1.0 (medium dashes), and crack density $\varepsilon = 0.02$, also with $k = 10.0$, $\varepsilon = 0.0242$ (short dashes) and 0.0034 (long dash-dot).

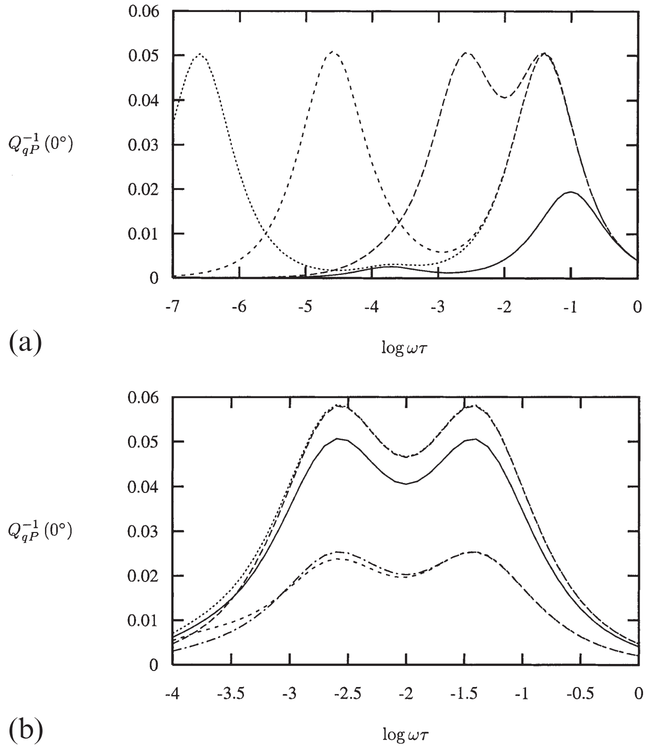

Figure 10. (a) The *P*-wave attenuation parameter Q_{qP}^{-1} for an incident wave perpendicular to the cracks as a function of non-dimensional frequency $\omega\tau$ with $P^m = 10^4$, for $P^k = 10^2$ (solid line), 10^4 (long dashes), 10^6 (medium dashes) and 10^8 (short dashes), with $\varepsilon = 0.02$ and $k = 10.0$. (b) The *P*-wave attenuation parameter Q_{qP}^{-1} for an incident wave perpendicular to the cracks as a function of non-dimensional frequency $\omega\tau$ for $P^k = 10^4$ and $P^m = 10^4$, with distribution parameter $k = 10.0$ (solid line), ∞ (long dashes) and 1.0 (medium dashes), and crack density $\varepsilon = 0.02$, also with $k = 10.0$, $\varepsilon = 0.023$ (short dashes) and 0.01 (long dash-dot).

A change in k is distinguishable from a change in ε, although only at higher frequencies (see Fig. 9b), where at low frequencies increasing k to infinity appears equivalent to increasing ε to 0.242 and decreasing k to 1.0 is almost equivalent to decreasing ε to 0.0034. The *P*-wave attenuation coefficient, Q_{qP}^{-1}, also shows similar behaviour for this model as it does for the variable aspect ratio model (see Fig. 10a). A change in the value of P^m would alter this figure marginally for the smaller values of P^k only.

The change in Q_{qP}^{-1} with a change in k or ε is illustrated in Fig. 10(b). We note that while we see a close correspondence between increasing k to infinity and increasing ε to 0.023, and also between decreasing k to 1.0 and decreasing ε to 0.01, the values of ε at which this correspondence occurs differ from those at which a similar correspondence occurs in ε_T (see Fig. 9b). As with the variable aspect ratio model, the peak in Q_{qP}^{-1} is seen to occur at the same frequency at which ε_T has a maximum gradient.

A variation in the *SH*-wave attenuation coefficient, Q_{qSH}^{-1}, is seen with a variation in P^m (Fig. 11a). It is seen that for large enough values of P^m, there is a second (small) peak in Q_{qSH}^{-1} perpendicular to the cracks. For $P^m = 10^4$, such that a second peak occurs, the variation in Q_{qSH}^{-1} with k and ε is given in Fig. 11(b). While we are able to match the height of the low-frequency peak resulting from a change in k by a corresponding change in ε, the existence and relative height of the higher-frequency peak enables us to distinguish between the two competing effects.

For lower values of P^m, at which this second, smaller peak does not occur, the effects of k and ε become indistinguishable. The peaks in Q_{qSH}^{-1} occur at the frequency at which γ_T has a maximum gradient, thus for smaller P^m when γ_T exhibits only one region of change (see Fig. 8b), there is only the one peak in Q_{qSH}^{-1}, while for larger P^m, Q_{qSH}^{-1} exhibits a second peak.

9 DISCUSSION

We have seen that for both the variable aspect ratio and the variable orientation models there exist critical (non-dimensional) frequencies in both the variation of Thomsen's parameters and the attenuation coefficients at which either a peak is reached or a transition is made from one value to another. The significance of these critical frequencies is their potential use in determining estimates of the unknown parameters within the model—ε, α_0, δ, k and τ; $\mathbf{n}^0$ can be determined as the direction corresponding to maximum attenuation. We rely, then, on the value of τ being such that the critical (non-dimensional) frequencies are attainable within the frequency range that can be achieved seismically ($1 < \omega < 10^4$ rad s^{-1}). Estimates of τ (Hudson *et al.*

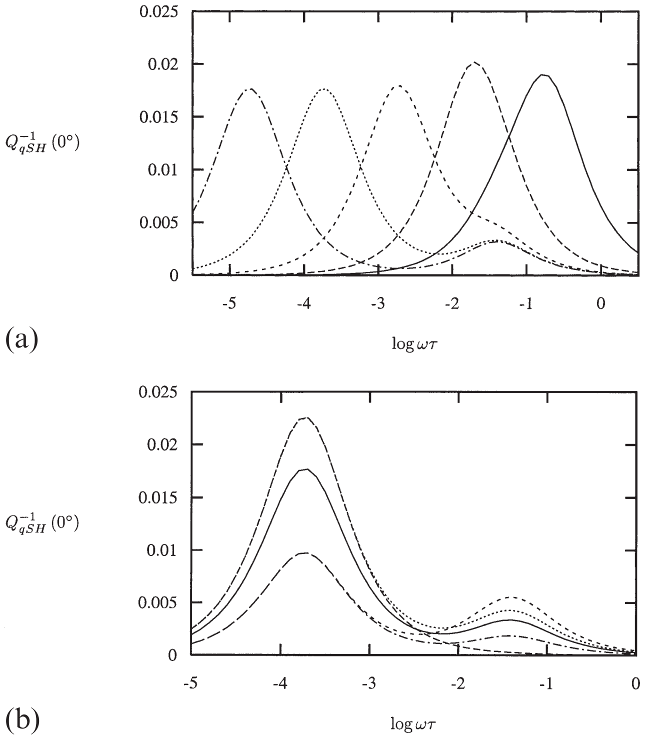

Figure 11. (a) The *SH*-wave attenuation parameter Q^{-1}_{qSH} for an incident wave perpendicular to the cracks as a function of non-dimensional frequency $\omega\tau$ for $P^m = 10$, (solid line), 10^2 (long dashes), 10^3 (medium dashes), 10^4 (short dashes) and 10^5 (long dash-dot), with $\varepsilon = 0.02$ and $k = 10.0$. (b) The *SH*-wave attenuation parameter Q^{-1}_{qSH} for an incident wave perpendicular to the cracks as a function of non-dimensional frequency $\omega\tau$ for $P^m = 10^4$, with distribution parameter $k = 10.0$ (solid line), ∞ (long dashes) and 1.0 (medium dashes), and crack density $\varepsilon = 0.02$, also with $k = 10.0$, $\varepsilon = 0.0255$ (short dashes) and 0.011 (long dash-dot).

1996; O'Connell & Budiansky 1977) lead us to believe that this is possible.

On consideration of either the variable aspect ratio or variable orientation model alone, it appears that we ought to be able to differentiate between the effects of ε and δ in the former, and ε and k in the latter, via Thomsen's parameters and the attenuation coefficients. Our ability to do this depends not only on the range of values of $\omega\tau$ at our disposal, but also on the values of P^k and P^m, both of which are inversely proportional to τ.

As might be expected, a very small variance in the aspect ratio distribution is not readily distinguishable from a similarly small variance in the orientation distribution. However, for larger variances, these effects do indeed become more distinguishable.

We could allow both the orientation and the aspect ratio to vary simultaneously, leading to an expression for the first-order correction to the elastic constants of the same form as eq. (73), but with a more elaborate expression for T_{krus}. For completeness, this form is given in Appendix E, although it is used nowhere within this paper.

Although the limit of fully aligned cracks of identical aspect ratio is a singular limit, in so far as its behaviour at low frequency is as if isolated, as opposed to undrained for non-aligned cracks, we see that this limit is not a significant one—there is no singularity in the behaviour of either Thomsen's parameters or the attenuation coefficients in this limit.

10 CONCLUSIONS

The model proposed by Hudson *et al.* (1996) for the transfer of fluid between connected cracks via non-compliant pores has been extended to allow for a continuous distribution of values of both crack orientation and aspect ratio. This more realistic model has the expected properties that at high frequencies the cracks behave as if isolated, while at low frequencies they behave as if undrained, and agree with the results of Brown & Korringa (1975). In the fully aligned limit they behave as if isolated at both high and low frequencies.

We looked separately at the cases of allowing the aspect ratio and orientation to vary, while keeping the other fixed, and studying the frequency dependence of Thomsen's parameters and the attenuation coefficients. For both models, we considered whether or not we were able to notice, and differentiate between, the effects of the variance of the distribution and the crack density of the model. Furthermore, we addressed the issue of differentiating between the effects of the variable aspect ratio and orientation.

We believe that it is possible to both notice and differentiate between the effects of the crack density and the variance of one or other of the models. Furthermore, we believe that there is some hope of distinguishing the effects of the variance of one model from those of the other.

Critically, however, there is a dependence upon the undetermined parameter corresponding to the relaxation time of pressure equalization between cracks, τ. Although estimates of this parameter have been made (Hudson *et al.* 1996; O'Connell & Budiansky 1977), a numerical investigation remains the subject of future work.

ACKNOWLEDGMENTS

I would like to thank Stephen J. Hay at Statoil, Norway, for permission to use the crack dimension data from his thesis (Hay 1988), John A. Hudson at DAMTP, University of Cambridge, for the content of Appendix A, and Enru Liu at the British Geological Survey for support and encouragement. The work was sponsored by the National Environment Research Council through project GST022305 as part of the thematic programme 'Understanding the micro-to-macro behaviour of rock fluid systems ($\mu 2M$)' and is published with the approval of the Director of the British Geological Survey.

REFERENCES

Brown, R.J.S. & Korringa, J., 1975. On the dependence of the elastic properties of a porous rock on the compressibility of the pore fluid, *Geophysics,* **40,** 608–616.

Carrier, G.F., Krook, M. & Pearson, C.E., 1983. *Functions of a Complex Variable, Theory and Technique,* Hod Books, New York.

David, C., Menéndez, B. & Darot, M., 1999. Influence of stress-induced and thermal cracking on physical properties and microstructure of La Peyratte granite, *Int. J. Rock Mech. Min. Sci.,* **36,** 433–448.

Fisher, N.I., Lewis, T. & Embleton, B.J.J., 1987. *Statistical Analysis of Spherical Data,* Cambridge University Press, Cambridge.

Fredrich, J.T. & Wong, T.-F., 1986. Micromechanics of thermally induced cracking in three crustal rocks, *J. geophys. Res.,* **91,** 12 743–12 764.

Gassmann, F., 1951. Elastic waves through a packing of spheres, *Geophysics,* **16,** 673–685.

Gibson, R.L. & Toksöz, M.N., 1990. Permeability estimation from velocity anisotropy in fractured rock, *J. geophys. Res.,* **95,** 15 643–15 655.

Hadley, K., 1976. Comparison of calaulated and observed crack densities and seismic velocities in Westerly granite, *J. geophys. Res.,* **81,** 3484–3494.

Hay, S.J., 1988. Permeability, past and present, in continental crustal basement, *PhD thesis,* University of Glasgow.

Hay, S.J., Hall, J., Simmons, G. & Russell, M.J., 1988. Sealed microcracks in the Lewisian of NW Scotland: A record of 2 billion years of fluid circulation, *J. geol. Soc. Lond.,* **145,** 819–830.

Homand-Etienne, F. & Houpert, R., 1989. Thermally induced microcracking in granites: characterization and analysis, *Int. J. Rock Mech. Min. Sci. Geomech. Abstr.,* **26,** 125–134.

Hudson, J.A., 1980. Overall properties of a cracked solid, *Math. Proc. Camb. Phil. Soc.,* **88,** 371–384.

Hudson, J.A., 1981. Wave speeds and attenuation of elastic waves in material containing cracks, *Geophys. J. R. astr. Soc.,* **64,** 133–150.

Hudson, J.A., 1986. A higher order approximation to the wave propagation constants for a cracked solid, *Geophys. J. R. astr. Soc.,* **87,** 265–274.

Hudson, J.A., Liu, E. & Crampin, S., 1996. The mechanical properties of materials with interconnected cracks and pores, *Geophys. J. Int.,* **124,** 105–112.

Keller, J.B., 1964. Stochastic equations and wave propagation in random media, *Proc. Symp. appl. Math.,* **16,** 145–170.

Mardia, K.V., 1972. *Statistics of Directional Data,* Academic Press, New York.

Menéndez, B., David, C. & Darot, M., 1999. A study of the crack network in thermally and mechanically cracked granite samples using confocal scanning laser microscopy, *Phys. Chem. Earth,* **A24,** 627–632.

Montoto, M., Martínez-Nistal, A., Rodríguez-Rey, A., Fernández-Merayo, N. & Soriano, P., 1995. Microfractography of granite rocks under confocal scanning laser microscopy, *J. Microscopy,* **177,** 138–149.

Nishizawa, O., 1982. Seismic velocity anisotropy in a medium containing orientated cracks—transversely isotropic case, *J. Phys. Earth,* **30,** 331–347.

O'Connell, R.J. & Budiansky, B., 1974. Seismic velocities in dry and saturated cracked solids, *J. geophys. Res.,* **79,** 5412–5426.

O'Connell, R.J. & Budiansky, B., 1977. Viscoelastic properties of fluid-saturated cracked solids, *J. geophys. Res.,* **82,** 5719–5735.

Peacock, S. & Hudson, J.A., 1990. Seismic properties of rocks with distributions of small cracks, *Geophys. J. Int.,* **102,** 471–484.

Pointer, T., Liu, E. & Hudson, J.A., 2000. Seismic wave propagation in cracked porous media, *Geophys. J. Int.,* **142,** 199–231.

Ross, S.M., 1989. *Probability Models,* 4th edn, Academic Press, San Diego.

Tapponnier, P. & Brace, W.F., 1976. Development of stress-induced microcracks in Westerly granite, *Int. J. Rock Mech. Min. Sci. Geomech. Abstr.,* **13,** 103–112.

Thomsen, L., 1986. Weak elastic anisotropy, *Geophysics,* **51,** 1954–1966.

Wong, T.-F., 1982. Micromechanics of faulting in Westerly granite, *Int. J. Rock Mech. Min. Sci. Geomech. Abstr.,* **19,** 49–64.

APPENDIX A: LOCAL DIFFUSION EQUATION

Let $\rho_{\rm f}^n$, ϕ_n and $p_{\rm f}^n$ be the fluid density, volume and pressure in the nth crack. The mass flow into the nth crack is

$$\dot{m}_n = \frac{\partial(\rho_{\rm f}^n \phi_n)}{\partial t}\,. \tag{A1}$$

Let $p_{\rm f}^m$ be the fluid pressure distribution due to unit pressure in the mth crack and zero in the rest. Let M_n^m be the associated flow into the nth crack. Then,

$$\dot{m}_n = \sum_m p_{\rm f}^m M_n^m = p_{\rm f}^n M_n^n + \sum_{m\neq n} p_{\rm f}^m M_n^m\,. \tag{A2}$$

Fluid mass is preserved and does not concentrate in the pores, so

$$\sum_m M_n^m = 0 \tag{A3}$$

or

$$\sum_{m\neq n} M_n^m = -M_n^n\,, \tag{A4}$$

thus

$$\dot{m}_n = -C\left[p_{\rm f}^n - \sum_{m\neq n} p_{\rm f}^m M_n^m \Big/ \sum_{m\neq n} M_n^m\right], \tag{A5}$$

where

$$C = \sum_{m\neq n} M_n^m = -M_n^n\,. \tag{A6}$$

We make the approximation

$$\sum_{m\neq n} p_{\rm f}^m M_n^m \Big/ \sum_{m\neq n} M_n^m \simeq p_{\rm f}\,, \tag{A7}$$

since it is clearly a weighted average of the pressure in the cracks (excluding the nth) and the weights decrease with distance, becoming negligible (probably) at several crack spacing lengths. Then

$$\dot{m}_n = -C\left[p_{\rm f}^n - p_{\rm f}(\mathbf{x}^n)\right], \tag{A8}$$

where $p_{\rm f}(\mathbf{x}^n)$ is an average of the $p_{\rm f}^n$ over a region $\mathscr{D}_n$ centred on $\mathbf{x}^n$, the centroid of the nth crack. Taking the average over $\mathscr{D}_n$,

$$\dot{m}(\mathbf{x}^n) = -C\left[p_{\rm f}(\mathbf{x}^n) - \sum_m w_n(\mathbf{x}^m) p_{\rm f}(\mathbf{x}^m) \Big/ \sum_m w_n(\mathbf{x}^m)\right], \tag{A9}$$

where w_n are weight functions. Thus,

$$\dot{m}(\mathbf{x}^n) = C \sum_m w_n(\mathbf{x}^m)[p_{\rm f}(\mathbf{x}^m) - p_{\rm f}(\mathbf{x}^n)] \Big/ \sum_m w_n(\mathbf{x}^m)\,. \tag{A10}$$

We identify

$$C = \frac{\phi_n^0 \rho_0}{\kappa_{\rm f}\tau}\,, \tag{A11}$$

a constant of appropriate dimensions, containing an unknown relaxation parameter, τ.

APPENDIX B: THOMSEN'S PARAMETERS

In the conventional condensed, two-subscript, 6×6 matrix notation, pairs of indices are represented as a single index: $ij\to p$, $kl\to q$, such that $11\to1$, $22\to2$, $33\to3$, $23\to4$, $13\to5$ and $12\to6$. We thus use the representation C_{pq}, rather than c_{ijkl} (eq. 1).

We make use of the anisotropy parameters defined by Thomsen (1986) for vertically transversely isotropic material,

$$\varepsilon_T \equiv \frac{C_{11} - C_{33}}{2C_{33}}\,, \tag{B1}$$

$$\delta_T \equiv \frac{(C_{13} + C_{44})^2 - (C_{33} - C_{44})^2}{2C_{33}(C_{33} - C_{44})}\,, \tag{B2}$$

$$\gamma_T \equiv \frac{C_{66} - C_{44}}{2C_{44}}\,, \tag{B3}$$

where the real part is assumed when the stiffnesses are complex.

We may use the wave speeds, eqs (C9) and (C10), to calculate two of these parameters,

$$\varepsilon_T = \frac{v_{qP}(90^\circ) - v_{qP}(0^\circ)}{v_{qP}(0^\circ)} \tag{B4}$$

and

$$\gamma_T = \frac{v_{qSH}(90^\circ) - v_{qSH}(0^\circ)}{v_{qSH}(0^\circ)}\,, \tag{B5}$$

to first order in ε.

APPENDIX C: WAVE SPEEDS AND *Q*

We make the assumption that the mean wave is a plane harmonic wave, $\mathbf{u} = \mathbf{b}e^{i\mathbf{k}\cdot\mathbf{x}}$ and substitute this into the time-harmonic equation of motion,

$$\frac{\partial}{\partial x_p} c_{ipjq} \frac{\partial u_j}{\partial x_q} + \rho\omega^2 u_i = 0\,, \tag{C1}$$

where ρ is the density of the matrix and ω the frequency of the propagating wave. We have

$$\left[\rho\omega^2 \delta_{ij} - c_{ipjq} k_p k_q\right] b_j = 0\,. \tag{C2}$$

The attenuation coefficient Q^{-1} is given by

$$Q^{-1} = 2\left|\frac{\mathscr{Im}(k)}{\mathscr{Re}(k)}\right|. \tag{C3}$$

For a given ω, we let $\mathbf{k} = \mathbf{k}^0 + \varepsilon\mathbf{k}^1$ and $\mathbf{b} = \mathbf{b}^0 + \varepsilon\mathbf{b}^1$ and equate coefficients of ε^0 and ε^1 in eq. (C2). Thus, at $\mathscr{O}(\varepsilon^0)$ and $\mathscr{O}(\varepsilon^1)$ we have

$$\begin{aligned} M_{ij} b_j^0 &= 0\,, \\ M_{ij} b_j^1 &= N_{ij} b_j^0, \end{aligned} \tag{C4}$$

where

$$\begin{aligned} M_{ij} &= \rho\omega^2 \delta_{ij} - c_{ipjq}^0 k_p^0 k_q^0\,, \\ N_{ij} &= c_{ipjq}^0 \left(k_p^0 k_q^1 + k_p^1 k_q^0\right) + c_{ipjq}^1 k_p^0 k_q^0\,. \end{aligned} \tag{C5}$$

The $\mathscr{O}(\varepsilon^0)$ term is just the isotropic result. To first order, the cracks have normal $(0, 0, 1)^{\mathrm{T}}$ and the rotational symmetry of the problem ensures that the material is transversely isotropic, so that, for a given ω, we can rotate the (x_1, x_2) plane such that

$$\mathbf{k}^0 = \frac{\omega}{v}(\sin\theta, 0, \cos\theta)^{\mathrm{T}} \tag{C6}$$

for some incident angle θ, where $v = v_P$ or v_S, corresponding to quasi-P (qP) waves, or quasi-S (qS) waves, respectively. For the qP wave, we have $\mathbf{b}_{qP}^0 = (\sin\theta, 0, \cos\theta)^{\mathrm{T}}$, while for the qS waves we have $\mathbf{b}_{qSV}^0 = (\cos\theta, 0, -\sin\theta)^{\mathrm{T}}$ or $\mathbf{b}_{qSH}^0 = (0, 1, 0)^{\mathrm{T}}$, corresponding to qSV and qSH waves, and we are free to choose the magnitude of $\mathbf{b}^0$. Pre-multiplication of the $\mathscr{O}(\varepsilon^1)$ term with $\mathbf{b}^0$ yields a single equation for the components of $\mathbf{k}^1$,

$$b_i^0 N_{ij} b_j^0 = 0\,. \tag{C7}$$

On the assumption that $\mathbf{k}^1$ is parallel to $\mathbf{k}^0$, this becomes an expression for the magnitude k^1 of $\mathbf{k}^1$.

The wave speeds, to first order, are given by

$$\frac{\omega}{\mathscr{Re}(k)} = v\,\mathscr{Re}\left(1 - \varepsilon\frac{v}{\omega}k^1\right), \tag{C8}$$

for $v = v_P$ or v_S, and we take the appropriate values of k^1. Thus, the normalized wave speeds are

$$\begin{aligned} \frac{v_{qP}}{v_P} = 1 + \frac{\varepsilon}{2(\lambda + 2\mu)} \\ \times \mathscr{Re}\left(\sin^4\theta\, C_{11}^1 + \cos^4\theta\, C_{33}^1 + \frac{1}{2}\sin^2 2\theta\, C_{13}^1 + \sin^2 2\theta\, C_{55}^1\right), \end{aligned} \tag{C9}$$

$$\frac{v_{qSV}}{v_S} = 1 + \frac{\varepsilon}{2\mu}\mathscr{Re}\left(\frac{1}{4}\sin^2 2\theta\left(C_{11}^1 + C_{33}^1 - 2C_{13}^1\right) + \cos^2 2\theta\, C_{55}^1\right), \tag{C10}$$

$$\frac{v_{qSH}}{v_S} = 1 + \frac{\varepsilon}{2\mu}\mathscr{Re}\left(\cos^2\theta\, C_{44}^1 + \sin^2\theta\, C_{66}^1\right). \tag{C11}$$

These are equivalent to Hudson (1981).

From eq. (C3), the attenuation coefficient is given by

$$Q^{-1} = \frac{2v}{\omega}\varepsilon\left|\mathscr{Im}(k^1)\right| \tag{C12}$$

to first order for $v = v_P$ or v_S and the appropriate k^1. Thus,

$$\begin{aligned} Q_{qP}^{-1} = \frac{\varepsilon}{\lambda + 2\mu}\bigg|\mathscr{Im}\bigg(\sin^4\theta\, C_{11}^1 + \cos^4\theta\, C_{33}^1 \\ + \frac{1}{2}\sin^2 2\theta\, C_{13}^1 + \sin^2 2\theta\, C_{55}^1\bigg)\bigg|, \end{aligned} \tag{C13}$$

$$Q_{qSV}^{-1} = \frac{\varepsilon}{\mu}\left|\mathscr{Im}\left(\frac{1}{4}\sin^2 2\theta\left(C_{11}^1 + C_{33}^1 - 2C_{13}^1\right) + \cos^2 2\theta\, C_{55}^1\right)\right|, \tag{C14}$$

$$Q_{qSH}^{-1} = \frac{\varepsilon}{\mu}\left|\mathscr{Im}\left(\cos^2\theta\, C_{44}^1 + \sin^2\theta\, C_{66}^1\right)\right|. \tag{C15}$$

APPENDIX D: NON-ZERO CONTRIBUTING TERMS OF Ω

We start by defining the integral

$$I_{m,n} = b(k)\int_0^{\pi/2} \sin^m\theta \cos^n\theta\, e^{k\cos^2\theta}\, d\theta\,. \tag{D1}$$

The components of Ω_{tkrlus} that contribute to T_{krus} (eq. 74) are

$$(\Omega_{111111}+\Omega_{211211})=\frac{3}{8}I_{3,2}+\frac{1}{8}I_{3,0}=(\Omega_{122122}+\Omega_{222222}), \quad \text{(D2)}$$

$$(\Omega_{112112}+\Omega_{212212})=\frac{1}{8}I_{3,2}+\frac{3}{8}I_{3,0}=(\Omega_{121121}+\Omega_{221221}), \quad \text{(D3)}$$

$$(\Omega_{113113}+\Omega_{213213})=\frac{1}{2}I_{1,4}+\frac{1}{2}I_{1,2}=(\Omega_{123123}+\Omega_{223223}), \quad \text{(D4)}$$

$$(\Omega_{111122}+\Omega_{211222})=-\frac{1}{8}I_{5,0}=-\Omega_{311322}, \quad \text{(D5)}$$

$$(\Omega_{111133}+\Omega_{211233})=-\frac{1}{2}I_{3,2}=(\Omega_{122133}+\Omega_{222233})=-\Omega_{311333}$$
$$=-\Omega_{322333}, \quad \text{(D6)}$$

$$(\Omega_{131131}+\Omega_{231231})=\frac{1}{2}I_{5,0}=(\Omega_{132132}+\Omega_{232232}), \quad \text{(D7)}$$

$$(\Omega_{133133}+\Omega_{233233})=I_{3,2}, \quad \text{(D8)}$$

$$\Omega_{311311}=\frac{3}{8}I_{5,0}=\Omega_{322322}, \quad \text{(D9)}$$

$$\Omega_{312312}=\frac{1}{8}I_{5,0}=\Omega_{321321}, \quad \text{(D10)}$$

$$\Omega_{313313}=\frac{1}{2}I_{3,2}=\Omega_{323323}=\Omega_{331331}=\Omega_{332332}, \quad \text{(D11)}$$

$$\Omega_{333333}=I_{1,4}, \quad \text{(D12)}$$

and those related to the above by the symmetries

$$\Omega_{tkrlus}=\Omega_{tkslur}=\Omega_{lurtks}=\Omega_{lustkr}. \quad \text{(D13)}$$

APPENDIX E: VARIABLE ASPECT RATIO AND ORIENTATION

For completeness, we give an expression for the first-order correction to the elastic constants derived by allowing both the aspect ratio and the orientation to vary while remaining independent of one another:

$$c^1_{ipjq}=-\frac{1}{\mu}c^0_{krip}c^0_{usjq}T_{krus}, \quad \text{(E1)}$$

where

$$T_{krus}=\left[(\delta_{t1}\delta_{l1}+\delta_{t2}\delta_{l2})\tilde{\mathscr{U}}_{11}+\frac{8}{3}\delta_{t3}\delta_{l3}(1-\nu)\frac{(1-i\omega\tau)F_1}{1-i\omega\tau\gamma_0}\right]\Omega_{tkrlus}$$
$$-\frac{8}{3}(1-\nu)\Pi_{kr}\Pi_{us}\left((\gamma_0-1)F_1-\frac{\kappa_{\rm f}}{\kappa}(F_2-F_1)\right)\frac{F_1}{1-i\omega\tau\gamma_0}$$
$$\times\left[\gamma_0F_1+\left(1-\frac{\kappa_{\rm f}}{\kappa}\right)(F_2-F_1)+i\omega\tau P^k(1-i\omega\tau\gamma_0)\right]^{-1}. \quad \text{(E2)}$$